Optics Letters

Multi-wavelength Yb:YAG/Nd^{3+}:YVO_4 continuous-wave microchip Raman laser

XIAO-LEI WANG,[1] JUN DONG,[1,*] XIAO-JIE WANG,[1] JIE XU,[1] KEN-ICHI UEDA,[2] AND ALEXANDER A. KAMINSKII[3]

[1]Department of Electronics Engineering, School of Information Science and Engineering, Xiamen University, Xiamen 361005, China
[2]Institute for Laser Science, University of Electro-Communications, 1-5-1 Chofugaoka, Choufu, Tokyo 182-8585, Japan
[3]Institute of Crystallography, Russian Academy of Sciences, Leninsky Prospekt 59, Moscow 119333, Russia
*Corresponding author: jdong@xmu.edu.cn

Received 10 June 2016; revised 4 July 2016; accepted 5 July 2016; posted 6 July 2016 (Doc. ID 268154); published 26 July 2016

Multi-wavelength continuous-wave (CW) Raman lasers in a laser diode pumped Yb:YAG/Nd^{3+}:YVO_4 microchip Raman laser have been demonstrated for the first time to our best knowledge. The multi-wavelength laser of the first Stokes radiation around 1.08 μm has been achieved with a Raman shift of 261 cm^{-1} for a-cut Nd:YVO_4 crystal corresponding to the fundamental wavelength at 1.05 μm. Multi-wavelength laser operation simultaneously around 1.05 and 1.08 μm has been achieved under the incident pump power between 1.5 and 1.7 W. Multi-wavelength Raman laser with frequency separation of 1 THz around 1.08 μm has been obtained when the incident pump power is higher than 1.7 W. The maximum Raman laser output power of 260 mW at 1.08 μm is obtained and the corresponding optical-to-optical conversion efficiency is 4.2%. Elliptically polarized fundamental laser and linearly polarized Raman laser were observed in an Yb:YAG/Nd:YVO_4 CW microchip Raman laser. The experimental results of linearly polarized, multi-wavelength Yb:YAG/Nd:YVO_4 CW microchip Raman laser with adjustable frequency separation provide a novel approach for developing potential compact laser sources for Terahertz generation.

OCIS codes: (140.3550) Lasers, Raman; (140.3480) Lasers, diode-pumped; (140.3580) Lasers, solid-state; (140.3615) Lasers, ytterbium; (290.5910) Scattering, stimulated Raman.

http://dx.doi.org/10.1364/OL.41.003559

Stimulated Raman scattering (SRS) is a very effective traditional method for frequency conversion with the rapid development of Raman media. The spectra obtained with SRS cover wide wavelength from infrared to ultra-violet regions. Since the first CW self-Raman laser utilizing a Nd^{3+}:$KGd(WO_4)_2$ (Nd:KGW) crystal was demonstrated [1], one promising application of the Raman laser is to generate continuous-wave (CW) dual-wavelength laser with a small wavelength separation [2,3], which has been potentially used to generate terahertz radiation for applications on spectroscopy, optical communication, biological diagnosis, and imaging [4,5]. Various vanadates (YVO_4 [6–9], $GdVO_4$ [10–12], $LuVO_4$ [13–15]) doped with Nd^{3+} or Yb^{3+} ions with excellent laser and Raman characteristics have been widely used in laser diode pumped self-Raman lasers. The a-cut Nd:YVO_4 crystal has been widely used as Raman medium to generate Raman laser with the strong Raman shift lines at 893 cm^{-1} or 840 cm^{-1} [16]. Pulsed Raman laser at 1097 nm has been generated in actively Q-switched c-cut Nd:YVO_4 self-Raman laser with 259 cm^{-1} Raman shift line [17]. Ytterbium ions doped laser materials with broad absorption bandwidth, high doping concentration, low quantum defect, and good thermal properties have been demonstrated to be favorable candidates for high power laser operation [18]. CW [19] and passively *Q*-switched [20–24] Yb-doped self-Raman lasers have been demonstrated by using Yb^{3+}:$KGd(WO_4)_2$ [19,20], Yb^{3+}:$KY(WO_4)_2$ [21,22], Yb:$KLu(WO_4)_2$ [23], and Yb^{3+}:YVO_4 [24] crystals as Raman gain media. However, the performance of the self-Raman lasers is restricted by severe thermal loading because the self-Raman crystals are used as laser gain media and Raman media simultaneously. A CW Raman laser with 261 cm^{-1} Raman shift line by using Yb:YAG crystal as gain medium and Nd:YVO_4 crystal as Raman medium provides more flexible selection of the Raman laser wavelengths.

In this Letter, a CW microchip Raman laser utilizing Yb:YAG crystal as gain medium and a-cut Nd:YVO_4 crystal as Raman medium with the Raman conversion from 1.05 to 1.08 μm corresponding to the Raman shift of 261 cm^{-1} for a-cut Nd:YVO_4 crystal has been demonstrated for the first time to the best of our knowledge. Multi-wavelength oscillation of the fundamental wavelength laser at 1.05 μm and Stokes radiation at 1.08 μm was obtained. The maximum Raman laser output power of 260 mW was achieved at the incident pump power of 6.28 W. The polarization states of the fundamental laser and Raman laser have been investigated.

The schematic diagram of the experimental setup for laser diode end pumped Yb:YAG/Nd:YVO_4 CW microchip Raman laser is shown in Fig. 1. A fiber-coupled 940 nm laser diode with a core diameter of 200 μm and numerical aperture of 0.22 was used as the pump source. Two lenses with 8 mm focal length were used to collimate and focus the pump beam on the Yb:YAG crystal rear surface. The focused pump beam diameter is 100 μm incident on the Yb:YAG surface after the optics coupling system. The laser gain medium used in the experiment was a 1.2-mm-thick, 10 at. % doped Yb:YAG crystal grown by the Czochralski method along ⟨111⟩ direction. One surface of the Yb:YAG crystal was coated with antireflection at 940 nm and high reflection at 1030 to 1100 nm to act as the rear cavity mirror, the other surface was coated with antireflection at 1030 to 1100 nm to reduce the intracavity loss. A 1-mm-thick a-cut Nd:YVO_4 crystal doped with 1 at.% Nd^{3+} ions was used as the Raman medium. The intracavity surface of the Nd:YVO_4 crystal was antireflection coated at 1030 to 1100 nm, and the other surface of Nd:YVO_4 crystal was specially designed as the output mirror with high reflection at the fundamental laser region (HR at 1030–1060 nm) and a slight transmission (about 0.4%) at 1080 nm. The Nd:YVO_4 crystal was tightly attached to the Yb:YAG crystal and was held with two copper blocks with a 3 mm diameter hole in the center. The cavity length is 2.2 mm. The laser experiment was operated at room temperature without actively cooling elements. The output power was measured with a Thorlabs PM200 power meter. The output spectra of the laser were measured with an Anritsu optical spectral analyzer (MS9740A).

The Yb:YAG/Nd:YVO_4 microchip Raman laser oscillates at a fundamental wavelength of 1050 nm when the incident pump power is higher than 0.9 W. The first Stokes laser at 1076 nm oscillates when the incident pump power increases up to 1.5 W. Figure 2 shows the evolution of the laser emitting spectra of the fundamental and Stokes laser wavelength for Yb:YAG/Nd:YVO_4 CW microchip Raman laser at different incident pump power. The fundamental laser oscillated at 1049.9 and 1052.6 nm wavelengths when the incident pump power was 0.92 W, as shown in Fig. 2(a). The frequency separation of multi-wavelength lines is about 0.8 THz for 1050 nm fundamental laser. The emission peak cross-section at 1030 nm is much higher than that at 1050 nm for Yb:YAG crystal. However, there is a reabsorption peak centered at 1030 nm due to the quasi-three-level nature of Yb:YAG material. The laser-oscillating threshold for fundamental laser at 1030 nm increases because of the significant reabsorption loss at 1030 nm in a high Q resonator for fundamental laser with highly reflective coating directly in the laser crystal and Raman crystal facets. Therefore, the fundamental laser at 1050 nm oscillates in high Q Yb:YAG/Nd:YVO_4 microchip laser resonator. When the incident pump power was increased above 1.5 W, the first Stokes laser oscillated at 1076 nm with full width at half-maximum of 0.03 nm. The first Stokes laser oscillating at 1076 nm is corresponding to the Raman shift of 261 cm^{-1} for a-cut Nd:YVO_4 crystal. At the same time, fundamental laser oscillated at 1053, 1056, and 1059 nm when the incident pump power was 1.51 W, as shown in Fig. 2(b). When the incident pump power was increased to 1.58 W, the Stokes laser oscillated at 1071, 1074.7, 1076, and 1078 nm while the fundamental laser still oscillated at three wavelengths of 1052.6, 1056, and 1059.4 nm, as shown in Fig. 2(c). With further increase of the incident pump power, the fundamental laser oscillated at 1052 and 1056 nm, while the Raman laser oscillated at 1072, 1075.5, 1079, and 1082 nm, as shown in Fig. 2(d). When the incident pump power was between 1.5 and 1.65 W, multi-wavelength oscillation around 1050 and 1080 nm was dominant, as shown in Figs. 2(b)–2(d). When the incident pump power is increased from 0.92 to 1.7 W, the oscillating wavelengths of the fundamental laser and the oscillating wavelengths of the Raman laser tend to shift to longer wavelength. The red-shift laser wavelength with the incident pump power is attributed to the temperature dependent emission spectra of Yb:YAG crystal [18]. The fundamental laser is more effectively converted to a Raman laser with 261 cm^{-1} Raman line, and only the first Stokes laser oscillates with further increasing the incident pump power when the incident pump power is higher than 1.7 W. The Raman laser oscillates at multi-wavelength lines around 1080 nm and the number of the oscillating wavelengths increase with the incident pump power, which is attributed to the multi-wavelength oscillation of Yb:YAG crystal at 1050 nm. The Raman laser oscillates at 1076.5, 1080, 1083.5, and 1087 nm for the incident pump power of 2.88 W, as shown in Fig. 2(e). The Raman laser oscillates at 1077.5, 1081, 1084, 1087.5, and 1091 nm for the incident pump power of 3.54 W, as shown in Fig. 2(f). The frequency separation of multi-wavelength lines is about 1 THz for 1080 nm Raman laser.

When the incident pump power is increased to 4.25 W, two new weak spectral lines of 1104 and 1123 nm (frequency separation is 4.6 THz) were observed, as shown in Fig. 3(a). The Raman laser oscillating at 1104 nm is corresponding to the second Stokes wavelength of the Raman shift of 261 cm^{-1} for the fundamental laser wavelength at 1050 nm. For the oscillation

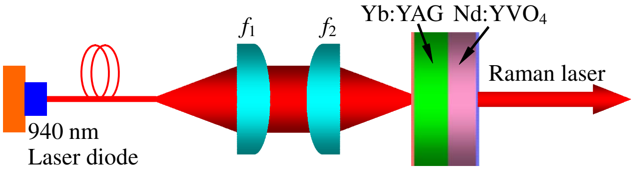

Fig. 1. Schematic diagram for a 940 nm laser diode end pumped Yb:YAG/Nd:YVO_4 CW microchip Raman laser. f_1 and f_2 are focus lenses with 8 mm focal length.

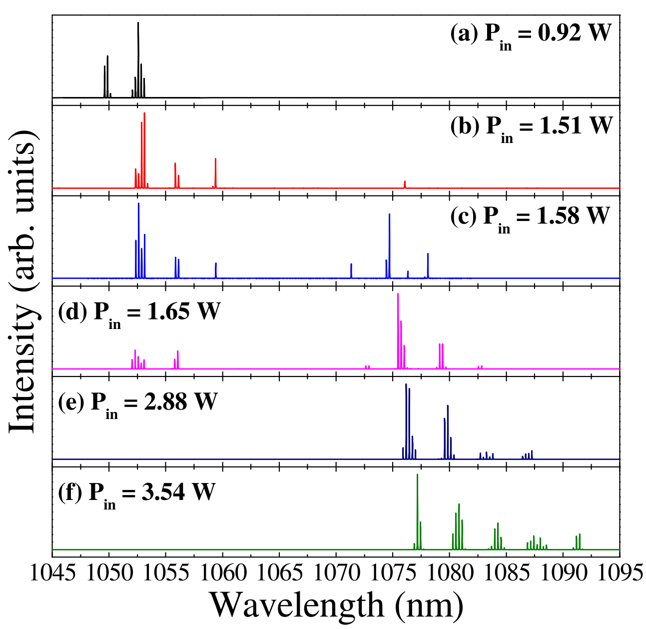

Fig. 2. Evolution of the laser emitting spectra of Yb:YAG/Nd:YVO_4 microchip Raman laser oscillating at fundamental laser and Stokes laser for different incident pump powers.

of 1123 nm, Raman laser is obtained by using the Raman shift of 261 cm^{-1} (to 1080 nm) combined with another Raman shift of 379 cm^{-1} (to 1123 nm) for the fundamental laser wavelength at 1050 nm. The oscillating wavelengths of second Stokes lasers at 1104 and 1123 nm is changed owing to the laser modes competition for the Raman gain. The second Stokes laser around 1123 nm disappears and only the second Stokes laser at 1108 nm oscillates when the incident pump power reaches up to 6.28 W, as shown in Fig. 3(b). The multi-wavelength Stokes lines of Yb:YAG/Nd:YVO_4 microchip Raman laser oscillate under high pump power due to low resonator losses for both fundamental laser and Raman laser provided by the high-reflectivity coatings directly to the surface of the crystals and the short cavity length of 2.2 mm used in the experiments. Therefore, the weak Stokes lines can reach the lasing thresholds for SRS. No Raman wavelength at 1158 nm corresponding to the 893 cm^{-1} Raman shift was observed in the experiment because the low reflectivity of the output surface of Nd:YVO_4 at this wavelength suppresses the 1158 nm Raman laser to reach the lasing threshold.

Both the fundamental lasers and Stokes lasers of Yb:YAG/Nd:YVO_4 CW microchip Raman laser oscillate in multi-longitudinal-mode at different incident pump power. The separation of longitudinal modes for fundamental laser is measured to be 0.26 nm and the separation of longitudinal modes for Stokes laser is measured to be 0.27 nm. The separation between longitudinal modes of fundamental and Raman laser are about 2 times of the free spectral range (FSR) of the Yb:YAG/Nd:YVO_4 CW microchip Raman laser. The FSR of Yb:YAG/Nd:YVO_4 CW microchip Raman laser is determined by the resonator filled with gain medium and Raman gain medium by $\Delta\lambda = \lambda^2/2L_C$ [25], where L_C is the optical length of the Raman laser resonator and λ is the wavelength of the fundamental laser or Raman laser. The FSR of the Yb:YAG/Nd:YVO_4 CW microchip Raman laser is 0.127 nm at 1050 nm and 0.133 nm at 1080 nm, respectively. The wide separation between the longitudinal modes is attributed to the thin intracavity Raman gain medium of 1-mm-thick Nd:YVO_4 crystal, which acts as a tilted etalon and selects the output longitudinal modes [25]. The linewidth (full width at half-maximum) of the fundamental or Raman laser mode was less than 0.03 nm, which was restricted by the resolution of available optical spectra analyzer.

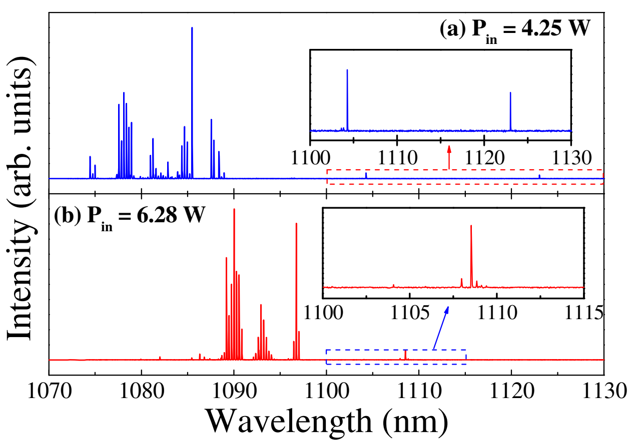

Fig. 3. Laser emitting spectra of a Yb:YAG/Nd:YVO_4 microchip Raman laser oscillating at first Stokes and second Stokes Raman lines.

Figure 4 shows the output power of the fundamental laser and Stokes laser with respect to the incident pump power. The pump power thresholds for the fundamental and Stokes laser wavelength were about 0.9 W and 1.5 W, respectively. The total output power increases linearly with the incident pump power when the incident pump power reaches the threshold of the fundamental laser. The slope efficiency is 4.7% with respect to the incident pump power. No saturation of the total output power was observed under the available pump power, indicating that the total output power can be further scaled by increasing the pump power. Simultaneous oscillating of the fundamental laser and first Stokes laser has been achieved in Yb:YAG/Nd:YVO_4 CW microchip Raman laser when the incident pump power was between 1.5 and 1.7 W. The typical fundamental laser and the first Stokes laser simultaneously oscillating spectra at different incident pump power were shown in Figs. 2(b)–2(d). The total output power of 26.4 mW was obtained at the incident pump power of 1.58 W, the output powers at fundamental laser wavelength and first Stokes laser wavelength were measured to be 11 mW and 15.4 mW, respectively. The maximum output power for Stokes radiation of 260 mW was obtained at the incident pumped power of 6.28 W, the corresponding optical-to-optical efficiency was 4.2%. The performance of the Yb:YAG/Nd:YVO_4 CW microchip Raman laser can be further improved by using longer Raman crystal and optimizing the coating parameters of both the laser gain medium and Raman crystal.

The polarization states of fundamental laser and Raman laser were also investigated by measuring the output power after the Glan–Thomson prism. The stable elliptically polarized fundamental laser and linearly polarized Raman laser were observed in Yb:YAG/Nd:YVO_4 CW microchip Raman laser. Figure 5 shows the typical polarization states of fundamental laser at the incident pump power of 0.92 W and the Raman laser at the incident pump power of 3.54 W of Yb:YAG/Nd:YVO_4 CW microchip Raman laser. The crystalline orientation dependent polarization states in the laser diode pumped Yb:YAG microchip laser have been investigated and found that the linearly, elliptically and circularly polarized states could be obtained by selecting different crystalline orientation in (111) plane [26–28]. Laser diode pumped Yb:YAG microchip lasers generally exhibit elliptical polarization state, while circular polarization and linearly polarization states are

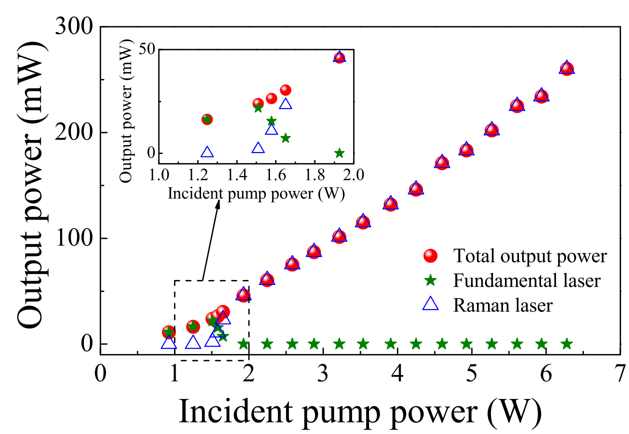

Fig. 4. Output power of Yb:YAG/Nd:YVO_4 CW microchip Raman laser versus the incident pump power.

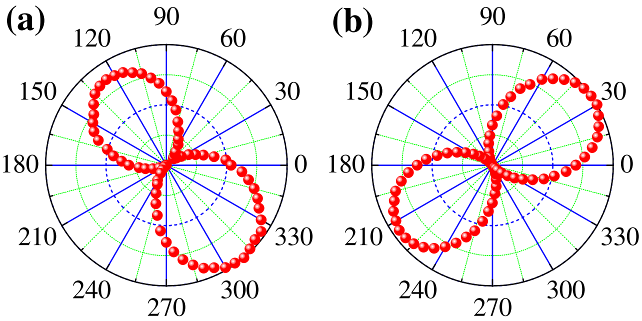

Fig. 5. Polarization states of laser diode pumped Yb:YAG/$Nd:YVO_4$ CW microchip Raman laser, (a) fundamental laser at the incident pump power of 0.92 W and (b) Raman laser at the incident pump power of 3.54 W.

generated only in the situation of the transition dipole moment of Yb:YAG crystal in (111) plane satisfying the three-fold D_2 symmetry in the YAG crystal [27]. The special orientations of ⟨111⟩ Yb:YAG crystal for linearly polarized laser output was not chosen in the Yb:YAG/$Nd:YVO_4$ CW microchip Raman laser experiment, therefore, stable elliptical polarized fundamental laser was observed when the incident pump power was lower than that for the Raman laser oscillation, as shown in Fig. 5(a) at the incident pump power of 0.92 W. Owing to the natural birefringence characteristic of the a-cut $Nd:YVO_4$ crystal, linear polarized Raman laser was observed when the incident pump power were highly sufficient to overcome the laser threshold of Raman laser. The linearly polarization state of Yb:YAG/$Nd:YVO_4$ CW microchip Raman laser is not changed with the incident pump power, as shown in Fig. 5(b) at the incident pump power of 3.54 W. The polarization direction of the linearly polarized Raman laser depends on the orientation of $Nd:YVO_4$ crystal when the $Nd:YVO_4$ crystal is rotated in Yb:YAG/$Nd:YVO_4$ CW microchip Raman laser, which also confirms that the linearly polarization state of Raman laser is determined by the birefringence characteristic of the $Nd:YVO_4$ crystal. The performance of Yb:YAG/$Nd:YVO_4$ CW microchip Raman laser could be further enhanced by carefully selecting the orientation of ⟨111⟩-Yb:YAG crystal to couple with the linearly polarized orientation of $Nd:YVO_4$ crystal. Multi-wavelength laser oscillation with frequency separation of about 1 THz in linearly polarized Yb:YAG/$Nd:YVO_4$ CW microchip Raman laser around 1.08 μm provides potential laser sources for developing THz radiation sources.

In conclusion, a laser diode end-pumped Yb:YAG/$Nd:YVO_4$ CW microchip Raman laser has been demonstrated for the first time to the best of our knowledge. Multi-wavelength oscillation of the fundamental laser around 1.05 μm and Stokes radiation around 1.08 μm was obtained under the incident pump power between 1.5 and 1.7 W. The maximum Raman laser output power of 260 mW was measured at the incident pump power of 6.28 W; the corresponding optical-to-optical efficiency is 4.2%. The linearly polarized Raman laser has been obtained in laser diode pumped Yb:YAG/$Nd:YVO_4$ CW microchip Raman laser. Multi-wavelength laser oscillation with adjustable frequency separation around 1.05, 1.08, and 1.11 μm in laser diode pumped Yb:YAG/$Nd:YVO_4$ CW microchip Raman laser opens a new window for designing a compact laser source for terahertz generation.

Funding. National Natural Science Foundation of China (NSFC) (61275143, 61475130); Program for New Century Excellent Talents in University (NCET) (NCET-09-0669).

Acknowledgment. X. L. Wang would like to thank Dr. S. C. Bai and M. M. Zhang for their help in experiments and discussion.

REFERENCES

1. A. A. Demidovich, A. S. Grabtchikov, V. A. Lisinetskii, V. N. Burakevich, V. A. Orlovich, and W. Kiefer, Opt. Lett. **30**, 1701 (2005).
2. K. Zhong, C. L. Sun, J. Q. Yao, D. G. Xu, X. Y. Xie, X. L. Cao, Q. L. Zhang, J. Q. Luo, D. L. Sun, and S. T. Yin, IEEE J. Quantum Electron. **49**, 375 (2013).
3. R. Akbari, H. T. Zhao, and A. Major, Opt. Lett. **41**, 1601 (2016).
4. J. B. Baxter and G. W. Guglietta, Anal. Chem. **83**, 4342 (2011).
5. C. B. Reid, E. Pickwell-MacPherson, J. G. Laufer, A. P. Gibson, J. C. Hebden, and V. P. Wallace, Phys. Med. Biol. **55**, 4825 (2010).
6. A. A. Demidovich, L. E. Batay, A. S. Grabtchikov, V. A. Lisinetskii, V. A. Orlovich, and A. N. Kuzmin, *Advanced Solid-State Photonics* (Optical Society of America, 2004), paper TuB9.
7. A. J. Lee, H. M. Pask, T. Omatsu, P. Dekker, and J. A. Piper, Appl. Phys. B **88**, 539 (2007).
8. Y. T. Chang, H. L. Chang, K. W. Su, and Y. F. Chen, Opt. Express **17**, 11892 (2009).
9. X. L. Li, A. J. Lee, H. M. Pask, J. A. Piper, and Y. J. Huo, Opt. Lett. **36**, 1428 (2011).
10. P. Dekker, H. M. Pask, and J. A. Piper, Opt. Lett. **32**, 1114 (2007).
11. P. Dekker, H. M. Pask, D. J. Spence, and J. A. Piper, Opt. Express **15**, 7038 (2007).
12. A. J. Lee, H. M. Pask, P. Dekker, and J. A. Piper, Opt. Express **16**, 21958 (2008).
13. A. Kaminskii, H. Rhee, H. Eichler, K. Ueda, K. Oka, and H. Shibata, Appl. Phys. B **93**, 865 (2008).
14. A. A. Kaminskii, M. Bettinelli, J. Dong, D. Jaque, and K. Ueda, Laser Phys. Lett. **6**, 374 (2009).
15. Y. Tan, X. H. Fu, P. Zhai, and X. H. Zhang, Laser Phys. **23**, 045806 (2013).
16. R. Li, R. Bauer, and W. Lubeigt, Opt. Express **21**, 17745 (2013).
17. S. Fan, X. Zhang, Q. Wang, Z. Liu, L. Li, Z. Cong, X. Chen, and X. Zhang, Opt. Commun. **284**, 1642 (2011).
18. J. Dong, M. Bass, Y. L. Mao, P. Z. Deng, and F. X. Gan, J. Opt. Soc. Am. B **20**, 1975 (2003).
19. M. T. Chang, W. Z. Zhuang, K. W. Su, Y. T. Yu, and Y. F. Chen, Opt. Express **21**, 24590 (2013).
20. A. A. Lagatsky, A. Abdolvand, and N. V. Kuleshov, Opt. Lett. **25**, 616 (2000).
21. A. S. Grabtchikov, A. N. Kuzmin, V. A. Lisinetskii, V. A. Orlovich, A. P. Voitovich, A. A. Demidovich, H. J. Eichler, and A. N. Titov, Quantum Electron. **33**, 165 (2003).
22. A. S. Grabtchikov, A. N. Kuzmin, V. A. Lisinetskii, V. A. Orlovich, A. A. Demidovich, M. B. Danailov, H. J. Eichler, A. Bednarkiewicz, W. Strek, and A. N. Titov, Appl. Phys. B **75**, 795 (2002).
23. J. H. Liu, U. Griebner, V. Petrov, H. J. Zhang, J. X. Zhang, and J. Y. Wang, Opt. Lett. **30**, 2427 (2005).
24. V. E. Kisel, A. E. Troshin, N. A. Tolstik, V. G. Shcherbitsky, N. V. Kuleshov, V. N. Matrosov, T. A. Matrosova, and M. I. Kupchenko, Appl. Phys. B **80**, 471 (2005).
25. W. Koechner, *Solid State Laser Engineering* (Springer-Verlag, 1999).
26. J. Dong, A. Shirakawa, and K. Ueda, Appl. Phys. Lett. **93**, 101105 (2008).
27. J. Dong, J. Ma, and Y. Y. Ren, Laser Phys. **21**, 2053 (2011).
28. J. Dong, G. Z. Xu, J. Ma, M. J. Cao, Y. Cheng, K. Ueda, H. Yagi, and A. A. Kaminskii, Opt. Mater. **34**, 959 (2012).